

MECHANICS OF BED INFORMATIONS

BY F. SENTÜRK *

Introduction

Let us consider a plane bed covered by a non-cohesive sediment of non-uniform grain size. It is possible to define a state of flow at which sediment particles will stay at their initial positions and thus no sediment movement exists on the bed. Also, a broad range of hydraulic conditions exists at which sediment particles are in motion, but no configurations can be formed. The movement of the particle is discontinuous; it begins, it is accelerated then decelerated and comes to an end. This process is repeated indefinitely. As a result of the phenomenon, the resistance of a movable bed to fluid motion is less than the resistance of a fixed plane bed.

As the upper limit of the above mentioned range is reached, configurations begin to appear. The jump and the rest of the solid particles are accentuated. Bed configurations develop rapidly and cover the bottom completely. The first stage presents the following characteristics:

1° When the characteristic grain size, D , of the sediment in motion is less than 0,5 mm, bed configurations appear only in one category which is generally called the "ripple stage". This same terminology will be used in this paper.

2° The resistance to the flow shows a jump when passing from a plane bed to a wavy bed. It de-

creases afterwards when the dimensionless parameter:

$$f = \frac{S^2 F_*}{S^2 R_w} \quad (1)$$

increases [1];

$S^2 F_*$ denotes the square of the Froude's number (*) related to the grain size and $S^2 R_w$ the square of the Reynolds number related to the fall velocity.

3° Only a certain thickness of the material forming the bottom is in motion. This layer is continuously mixed up and it slides over a certain plane which presents the initial mean slope of the bottom (Fig. 1) that is as if the material is rolling over a solid surface having the slope S .

4° The celerity of the configurations is higher than the velocity of solid particles. This is an important property. When f increases the celerity of configurations decreases. There exists a state at which the celerity of the configurations is equal to the velocity of the grains. At that particular state, the configurations are washed out and a plane bed results. For bigger values of (f) the celerity of bed configurations is negative. These configurations are called anti-dunes.

5° The fact that the velocity of sand particles is smaller than the celerity of the configurations is part of the general law of motion in a natural flow.

If we consider the motion of a single particle, we

$$(*) \quad S^2 F_* = \frac{\tau_0}{\bar{\omega}' D} = \frac{\rho U_*^2}{\bar{\omega}' D} = \frac{\bar{\omega}}{\bar{\omega}'} \frac{U_*^2}{gD}$$

U_*^2/gD has the form of Froude's number. Therefore it will be called Froude's number related to the grain size.

* Dr. of Toulouse University; Head, General Directorate of Turkish State Hydraulic Works, Research Department; Professor of Civil Engineering Robert College, Istanbul, Turkey.

can see that it rolls over the surface of a ripple and is rejected from the top of it towards downstream. The grain can follow three different paths according to its size (Fig. 2).

- *Fine particles* : Are carried away by the flow and fall on the surface of another ripple (Fig. 2, particle 1) or are carried upstream by the return flow;
- *Medium size particles* : Fall to the closer region to the wave front. This, in general, is the explosion region of turbulence. The particle is then transferred to the upstream slope of the initial configuration, (Fig. 2, particle 2);
- *Large size particles* : Are transported by the flow and fall directly from the top of the configuration into the trough between two ripples, (Fig. 2, particle 3).

The turbulence is so violent that active erosion takes place on the upstream end of a ripple and the eroded material is transported upstream towards the preceding configuration. Therefore, these sand grains are added to the downstream slope of the configuration which precedes the first wave. The velocity of the configuration increases though the velocity of the particles in motion decreases relatively. It was found that in a particular case, the velocity of the configuration was about three times larger than the velocity of the grains in motion. The explosion region of the turbulence is not steady. It is in a perpetual motion.

The phenomenon described above is modified by the segmentation of configurations.

The turbulence regenerated by a single sand wave divide the configuration immediately downstream into two. The celerity of the newly formed wave is higher than the original, because of its small height. It continues its way up the back of the next configuration and dies on the top of it. Therefore, the delayed grains put in motion from the upstream end of a wave will be captured by the new configuration though half of it continues its way without any danger to be reached by the delayed sand particles. This is the second and important reason of the difference in velocity between waves and grains.

Let us consider Figure 3. Figure 3 *a* shows the profile of a normal bed configuration. In state 3 *b*, coarser materials are transported upstream, though finer materials are pushed downstream. The slope of the downstream end of the wave becomes steeper than in 3 *a*. This is natural because coarse mate-

rials act as a butress and prevent the slope from sliding. Case 3 *c* gives an illustration of this particular case. The movement of sediment being continuous, the slope becomes sharper and a sudden "sliding" occurs, this is once more case 3 *a*. The complete cycle continues as explained above. The double movement of the sediment and the wave are the reasons of a particular sediment sorting (Fig. 3 *c*). Sediment particles of the same size are grouped in layers which alternate with other layers during the movement of the sediment, at the bottom of the channel. A close consideration of Figures 3 *b*, 3 *c* and 3 *a* show this fact. Dye is used to visualise the phenomenon. In a given interval of time the distances travelled by coloured water in different layers can be followed from Figure 6. The layers themselves are visible on the same figure.

In the ripple stage, a characteristic wave is taken as a specimen and it is shown in Figures 4 and 5. This particular shape will be called, "rose petal". Figure 4 shows clearly a well formed petal and Figure 5 shows the general aspect of the channel with bottom covered with continuous rose petals.

The geometry of petals is variable. The downstream slope changes continuously. It was found during an experiment performed by sand No. 2 (Table 1) that this variation was between 42° and 52° with the horizontal. In the case of dunes, the angle of the downstream slope with the horizontal is approximately constant and equals 33°. The angle of internal friction of this material was found to be equal to 35°.

Resistance of bed configurations to the flow

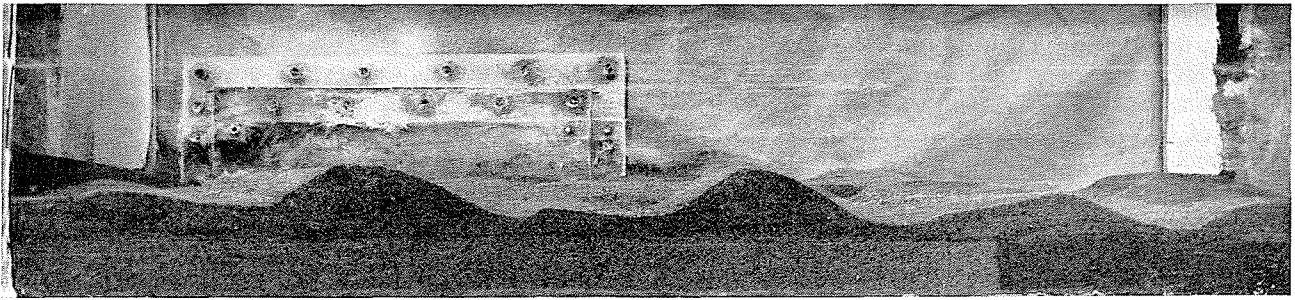
The resistance of a bed covered by a loose material is a complex phenomenon. We will try to describe it according to a large number of observations made on laboratory flumes. When a flow takes place on a plane fixed bed, the hydraulic radius increases with discharge. If a movement of particles begins though the bottom stays unchanged, say plane, a decrease in the hydraulic radius can then be observed (Fig. 7). That means a decrease in the resistance of the flow.

The phenomenon was observed by many hydraulicians working on the same subject [2]. When the bottom is covered by configurations, the resis-

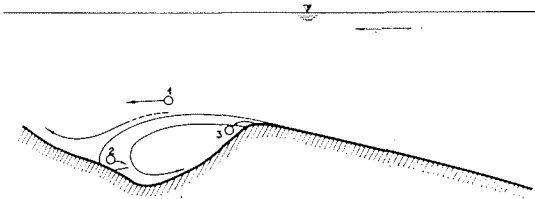
Table 1

Characteristics of the tested materials

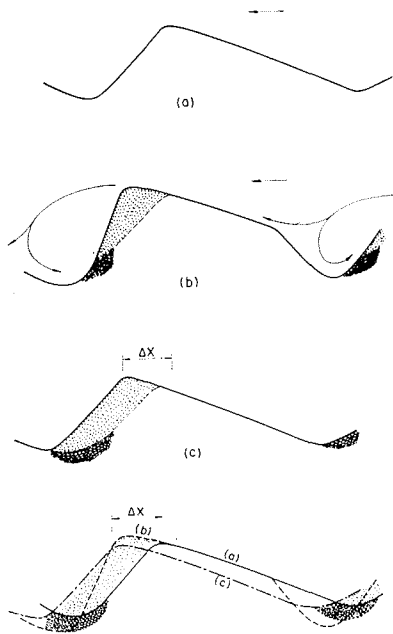
NATURE OF THE MATERIAL	D ₀₅ (mm)	D _m (mm)	D ₆₅ (mm)	D ₉₀ (mm)	\bar{w}' (t/m ³)	W ₀₅ (m/s)	W ₉₀ (m/s)
Pumice.	0,76	0,87	0,96	1,13	0,41	0,06	0,07
Sand No. 2.	0,34	0,40	0,42	0,55	1,61	0,05	0,06
Sand No. 3.	0,65	0,76	0,84	1,05	1,161	0,13	0,14
Plastics.		3			0,05		0,033
Sand No. 4.	2,20	2,80	3,20	4,20	1,53	0,32	0,29



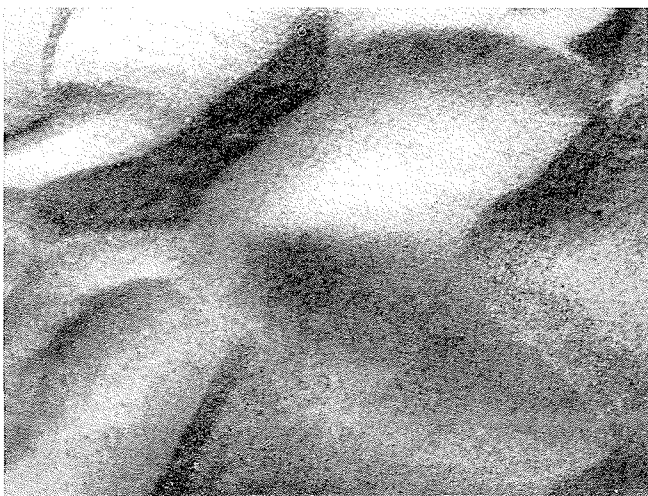
1/



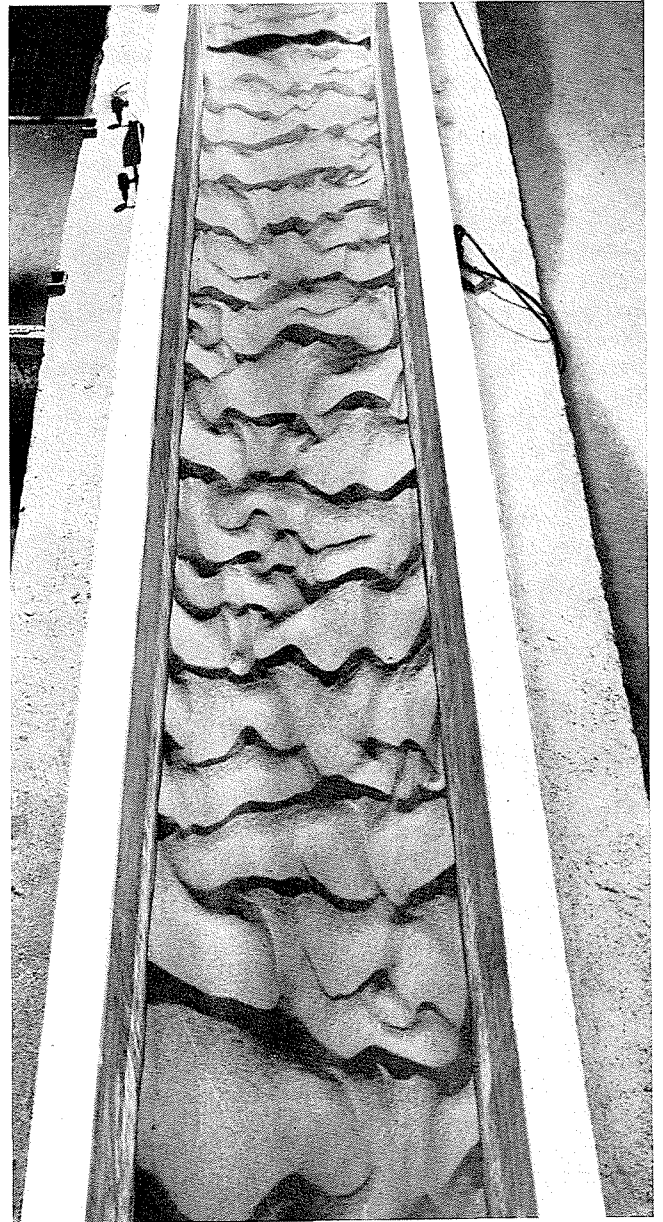
2/



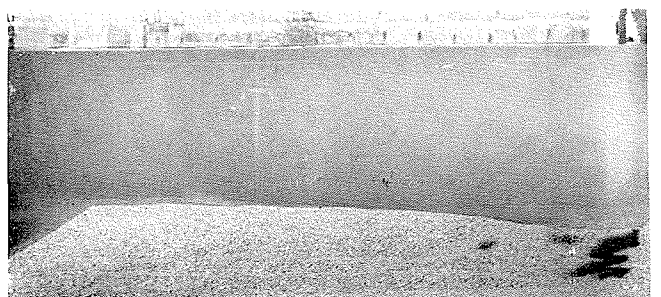
3/



4/



5/



6/

tance to the flow shows a jump and increases suddenly in certain cases. In other cases, a continuous increase takes place up to a critical state. This is a function of the grain size moving on the bottom of the channel. It will be shown that a category of configurations causing a decrease of resistance to the flow with increasing values of hydraulic conditions exists. This category is called, "ripples".

A new category of configurations can be defined according to the typical resistance they regenerate. This form is similar to ripples and the criteria given by Liu [3] range them in the category of ripples. However, the resistance they regenerate is somewhat different. It is a natural continuation of a plane bed resistance and it increases with the increasing values of the hydraulic conditions. This category of configurations will be called anti-ripples.

A critical value of the grain size separates the ripples from the anti-ripples. That means that ripples and anti-ripples can not be formed simultaneously with a given bed material. Both ripples and anti-ripples change their characteristics for a given critical value of the hydraulic properties and range themselves in a new category called dunes, which presents the property of "an increase of resistance

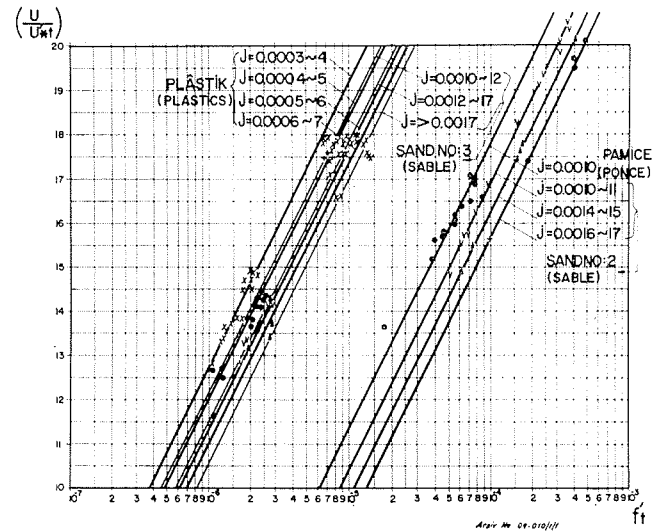
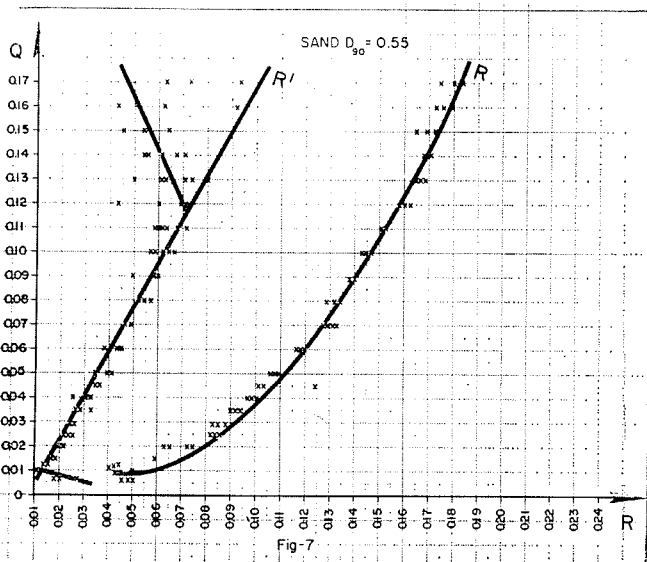
with increasing values of the hydraulic conditions". For dunes, ripples and anti-ripples, the flow is sub-critical. At critical flow, the bottom becomes plane once more and no configurations exist. In case of super critical flow, new configurations appear on the bed and travel upstream. These are called anti-dunes.

Mathematical approach to the computation of resistance of flow

General considerations.

As it was shown previously, a double movement exists at the bottom, the movement of single sand particles and the movement of bed configurations. It is natural to analyse their resistances separately for those two different items.

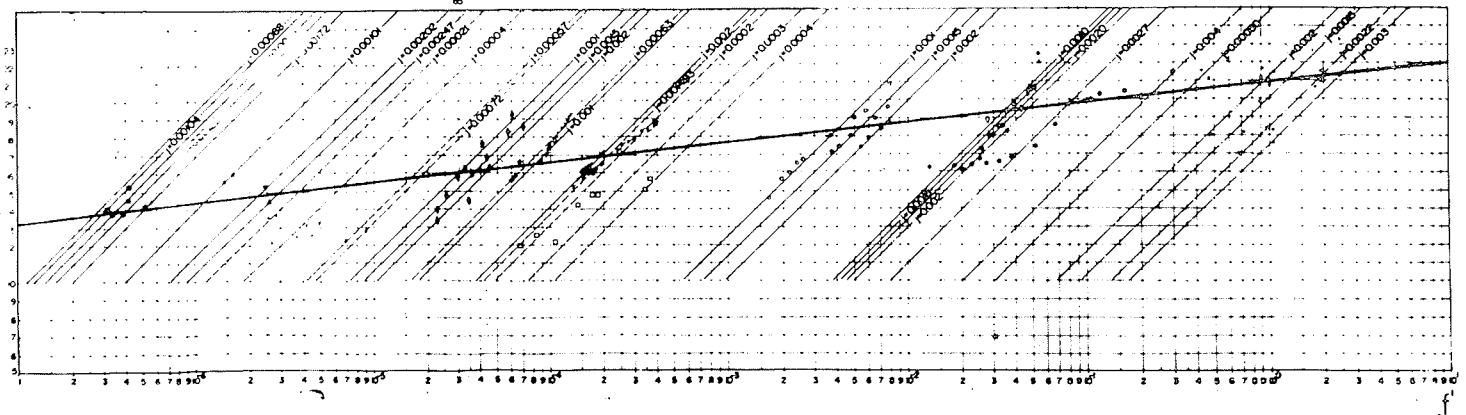
Einstein, thinking in the same way [4], has given a method of approach to the problem. His basic principles are retained in this study, but the resis-



7/

8/

- Faulner Q₀0.36mm
- Faulner Q₀0.21mm
- Brooks Q₀0.15mm
- Vanoni Q₀0.091mm
- Vanoni Q₀0.19mm
- Brooks Q₀0.094mm
- W Shen Q₀0.86mm Sable III
- F Sentürk Q₀1.72
- Laurene Q₀0.47mm
- Vanoni Q₀0.155mm
- S Atsoy
- W Shen Q₀3.17mm Sable II
- W Shen Q₀1.27mm Sable I



9/

tance due to bed configurations is defined similarly to the resistance due to sand particles. Let us consider a parameter which will be shown by "f":

$$f = \frac{\tau_0/\bar{\omega}' D}{W^2 D^2/\nu^2} \quad (1)$$

This is the friction parameter "f" where: τ_0 : shear stress at the bottom; $\bar{\omega}'$: specific weight of the sediment in motion weighed under water; D: characteristic diameter of the sediment in motion; W: settling velocity of the sediment particle of diameter D and specific weight $\bar{\omega}'$; ν : kinematic viscosity. "f" is a dimensionless number which is a quotient of two other dimensionless numbers. The first one can be related to the equilibrium of a particle under two distinct forces: the inertial and the gravitational forces. And the second enters in the definition of the drag coefficient C_D . "f" can then be attributed to the equilibrium or the movement of a sand particle. It is possible to derive it by the movement of a solid particle in stagnant water. Assuming, as it was previously done by Einstein [4], that the total hydraulic radius R can be divided into two parts, such as:

$$R = R' + R'' \quad (2)$$

where R' is the hydraulic radius related to the sand grains and R'' is the hydraulic radius related to bed configurations. It then becomes possible to write:

$$U_* = \sqrt{gR'j} \quad (3)$$

$$U''_* = \sqrt{gR''j} \quad (4)$$

$$U_*^2 + U''_*^2 = U_*^2 \quad (5)$$

In order to eliminate the wall effect, it is possible to compute these values specifically at the bottom, and obtain:

$$U'_{*t} = \sqrt{gR'_tj} \quad (6)$$

$$U''_{*t} = \sqrt{gR''_tj} \quad (7)$$

where: U_* : friction velocity related to grains; U'_{*t} : friction velocity related to grains and measured at the bottom of the bed; U''_{*t} : friction velocity related to bed configurations; U''_{*t} : friction velocity related to bed configurations and measured at the bottom of the bed, g: gravitational acceleration, j: hydraulic slope, U_* : friction velocity, R'_t : hydraulic radius related to sand grains and measured at the bottom, R''_t : hydraulic radius related to bed configurations and measured at the bottom.

The same way of thinking can be applied to the friction parameter f' , f'' , f'_t , f''_t . In fact, "f" can be written as:

$$f = \frac{R}{D_{35}} \frac{D_{65}}{D_{65}} \frac{\bar{\omega}}{\bar{\omega}'} \frac{j}{W_{65}^2 D_{65}^2/\nu^2} = K \frac{R}{D_{65}} \quad (8)$$

and:

$$f' = K \frac{R'}{D_{65}} \quad (9)$$

$$f'_t = KR'_t/D_{65} \quad (10)$$

$$f'' = KR''/D_{65} \quad (11)$$

$$f''_t = KR''_t/D_{65}$$

Variation of the resistance due to sand grains.

It is interesting to follow the variation of U/U'_{*t} , as a function of (f'_t), (U) being the mean velocity of the flow. Figure 8 shows the results obtained from experiments performed in a flume 90 cm wide at the Research Center in Ankara, Turkey.

Other data collected from published results are used in order to prepare Figure 9, which shows the same result as obtained from Figure 8. The plottings on a semi-log paper define straight lines parallel to a given direction with an equation in the form given below:

$$\frac{U}{U'_{*t}} = a' + b' \log f'_t \quad (12)$$

or:

$$\frac{U}{U'_{*t}} = a' + b' \log \frac{R'_t}{D_{65}} \frac{\bar{\omega}}{\bar{\omega}'} \frac{D_{65}}{D_{35}} \frac{j}{S^2 R_w} \quad (13)$$

where:

$$S^2 R_w = \left(\frac{W_{65} D_{65}}{\nu^2} \right)^2$$

Eq. (13) can be written as:

$$\frac{U}{U'_{*t}} = a' + b' \log \left(\frac{D_{65}}{D_{35}} \frac{\bar{\omega}}{\bar{\omega}'} \frac{j}{S^2 R_w} \right) + b' \log \frac{R'_t}{D_{65}} \quad (14)$$

and:

$$\frac{U}{U'_{*t}} = A' + b' \log \frac{R'_t}{D_{65}} \quad (15)$$

with:

$$a' + b' \log \frac{D_{65}}{D_{35}} \frac{\bar{\omega}}{\bar{\omega}'} \frac{j}{S^2 R_w} = A'$$

The form of equation (15) is similar to that given by Keulegan [5].

$$\frac{U}{U_*} = 6,00 + 5,75 \log \frac{R}{k} \quad (16)$$

If equation (15) is written for a very wide plane bed, it becomes possible to compare (15) with (16). And:

$$a' + b' \log \frac{D_{65}}{D_{35}} \frac{\bar{\omega}}{\bar{\omega}'} \frac{j}{S^2 R_w} = 6.00 \quad (17)$$

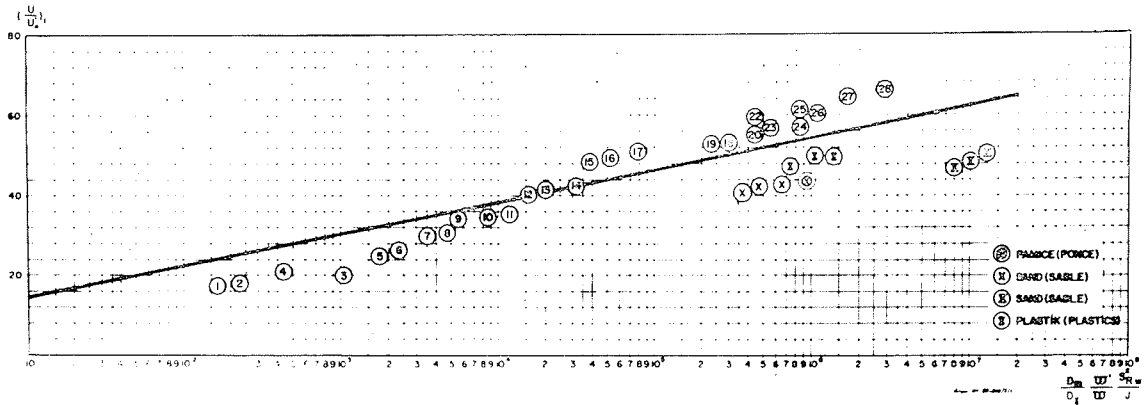
It was possible to check the above relation.

When A' stays constant, a certain variation in R'_t leads to a variation in U/U'_{*t} ; only one straight line is obtained. When j changes also, the straight line is translated and for different values of "j" it becomes possible to reach a family of straight lines. The same is true for the variation of the specific weight and the temperature of the liquid in motion. The sediment grading presents also a certain importance in the translation of the representative straight lines. The coefficient "b'" is a function of the constant coefficient defined by Von Karman. Different values of "b'" were found during the experiments but the mean value of it is equal to:

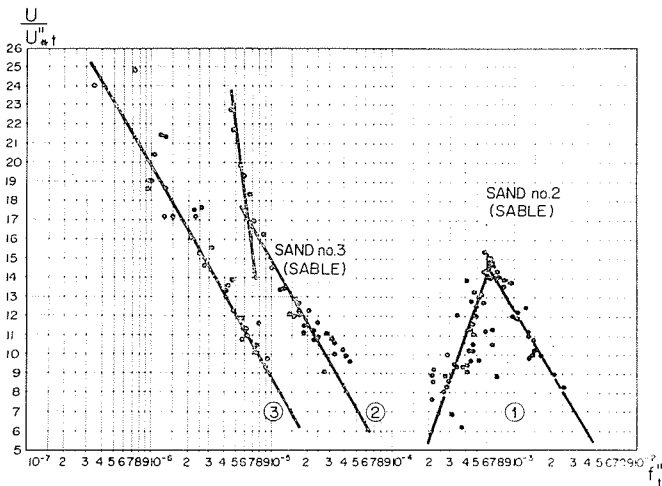
$$b' = 6.50 \quad (18)$$

in the range of experiments performed in the laboratory.

When plastics are used as solid material, the values of "b'" are more than 6.5. The exact defi-



10/



11/

dition of the straight lines required the determination of the variation of A' . An experimental study has given this variation (Fig. 10).

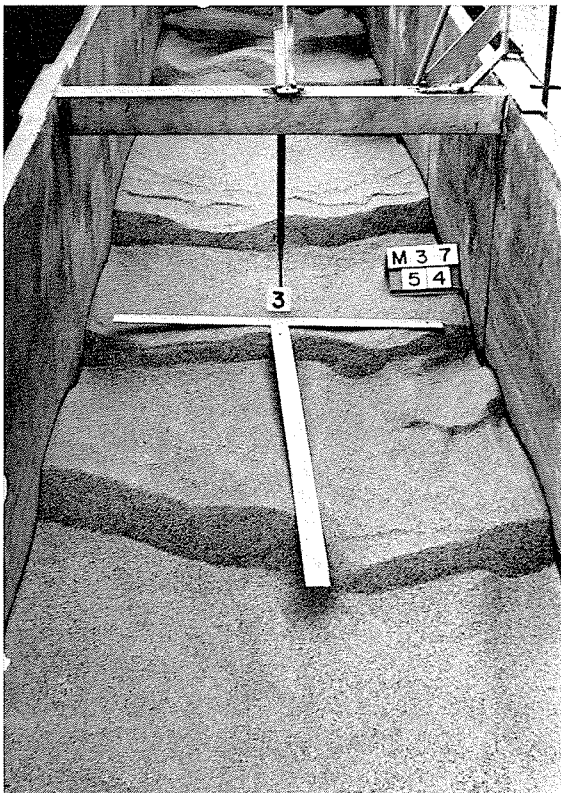
Consider equation (12). For:

$$f'_t = 1, \frac{U}{U'_{*t}} = a' = \left(\frac{U}{U'_{*t}} \right)_1$$

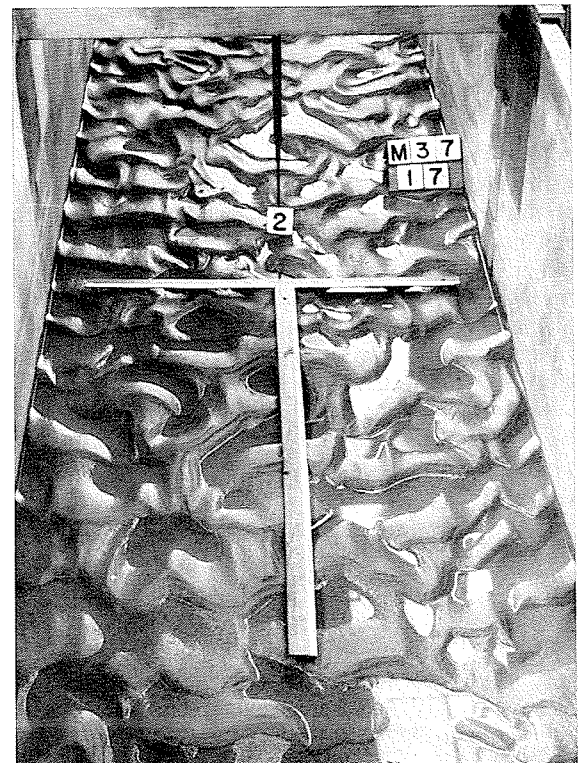
This value is plotted on Figure 10 as the ordinate and as abscissa the parameter:

$$\frac{D_{35}}{D_{65}} \frac{\bar{\omega}'}{\bar{\omega}} \frac{S^2 R_w}{j}$$

which is called the *spacing parameter*, is used. Each straight line of Figures 8 and 9 is represented on Figure 10, by a single point which is the intercept of the lines. It is possible to see



12/



13/

that a semi-logarithmic plotting leads to a straight line which can be represented by equation (19).

$$\left(\frac{U}{U''_{*t}}\right)_1 = 6.00 + 4.50 \log \frac{D_{35} \bar{\omega}}{D_{65} \bar{\omega}} \frac{S^2 R_w}{j} = a \quad (19)$$

If studied carefully, Figure 10 leads to a very good approximation though the experiments done by different hydraulicians were undertaken under different conditions. Introducing this value in Eq. (14);

$$\frac{U}{U''_{*t}} = 6.00 - 2 \log \frac{D_{35} \bar{\omega}}{D_{65} \bar{\omega}} \frac{S^2 R_w}{j} + 6.5 \log \frac{R'_t}{D_{65}} \quad (20)$$

is obtained as the equation of a flow with movable bed related to sand grains.

When:

$$\frac{D_{35} \bar{\omega}}{D_{65} \bar{\omega}} \frac{S^2 R_w}{j} = 1$$

Eq. (20) is transformed to:

$$\frac{U}{U''_{*t}} = 6.00 + 6.5 \log \frac{R'_t}{D_{65}} \quad (21)$$

which is very similar to the equation derived by Keulogan [5]. When the bottom is fixed, then 6.5 is reduced to 5.75 and the flow equation for a very wide channel is obtained as:

$$\frac{U}{U_*} = 6.00 + 5.75 \log \frac{R}{k_s}$$

Variation of the resistance due to bed configurations.

Equation (14) presents an interesting form which can be transposed directly to bed configurations:

$$\frac{U}{U''_{*t}} = a'' + b'' \log \left(\frac{D_{65} \bar{\omega}}{D_{35} \bar{\omega}} \frac{j}{S^2 R_w} \right) + b'' \log \frac{R'_t}{D_{65}} \quad (22)$$

This relation may reproduce the resistance of bed configurations to the flow. Experimental methods will be used in order to show the validity of (22). It is worthwhile to point out that the resistance of a plane bed is unique. This means that a single law can represent it. Bed configurations are classified in four groups. Principally, each category may have its own law of resistance. In this paper, only three of those groups are investigated and special laws are determined relative to each category. Therefore, different values pertaining the coefficient a'' and b'' may be determined as a consequence of this study.

Determination of: $\frac{U}{U''_{*t}} = f(f''_t)$.

When the physical properties of a movable material are given, Eq. (14) is completely determined. This statement assumes the knowledge of the hydraulic slope. If grading of the bed material is considered, it is possible to obtain the following bed forms at the bottom:

- 1° ripples first, dunes afterwards;
- 2° anti-ripples first and dunes afterwards;
- 3° only dunes.

Let us consider Figure 11. Case 1 is shown on it with the broken line 1, case 2 by line 2 and case

3 by line 3. If it is assumed that Eq. (23) is valid, then:

$$\frac{U}{U''_{*t}} = A'' + B'' \log f''_t \quad (23)$$

In fact an experimental approach has already given the proof of such a property. The straight line 3 represents dunes. The slope is negative. Figure 12 represents a characteristic view from such a category of configurations. In this case the only configurations which can be formed at the bottom are dunes and anti-dunes. As anti-dunes are not considered in this study, the diagram shows only the dunes. It is possible to check that the increasing values of f''_t correspond to the decreasing values of U/U''_{*t} , that is the resistance due to this category of bed forms increases with increasing values of f''_t .

This case can only be obtained when the diameter of the grains are greater than a given value which is approximately equal to 3,5 mm. The broken line 2 (Fig. 11) shows a continuous increase in the resistance for increasing values of f''_t . The point of intersection of the two straight lines is not completely determined. The broken line 1 shows a straight line with a positive slope, and another one with negative slope. An indeterminate transition region exists between those two segments. The line with positive slope represents ripples. Figure 13 shows a characteristic view of ripples. The upper reach of line 2 corresponds to anti-ripples and Figure 14 shows an example of them. It seems that the main reason of this classification rests on the sediment grading. Table 2 summarizes different limits already obtained from experiments.

Table 2 <i>Limit diameters of grains for different bed configurations</i>	
CATEGORY OF BED CONFIGURATIONS	LIMIT DIAMETER (mm)
Dunes.	D > 3 mm
Anti-ripples.	0.55 mm < D < 1.50 mm
Ripples.	D < 0.55 mm

When ripples and dunes are formed on a movable bottom, the resistance decreases first and increases afterwards. In that case, the same resistance can be obtained for two different values of (f''_t). The experiments done have shown that no sudden jump of resistance exists between two categories of configurations except for the beginning of ripples. The transition is smooth and gradual; especially for anti-ripples and dunes. In the case of ripples, the rose petals are grouped in such a way that they can be taken for ripples and dunes. This state of the bottom gives plottings on the top of the broken line 1 in Figure 11. An indetermination exists in fact, and it is difficult to say that the resistance regenerated by ripples is smaller or greater than the resistance regenerated by dunes.

It is known that an hysteresis phenomenon exists related to bed resistance [6]. It can be seen when

bed configurations change their form [7]. A double interference causes a continuous variation of the slope and the depth of water. Therefore, it becomes difficult to obtain a uniform flow beginning from plane bed. The phenomenon pointed out above, gives a picture of the natural variation of the bottom and the hydraulic properties according to that variation. Figure 15 gives the result of various experiments done in the Research Center.

Different kinds of configurations have given their characteristic straight lines. A single broken line is shown on the diagram for simplicity instead of a family of lines. The equations derived from these experiments are given below:

— dunes:

$$\frac{U}{U''_*} = A_1 - B_1 \log f''_t \quad (24)$$

$$A_1 = -96 + 11 \log C \quad (25)$$

$$B_1 = 11 \quad (26)$$

$$C = \frac{D_{35}}{D_{65}} \frac{\bar{\omega}}{\bar{\omega}} \frac{S^2 R_w}{j} \quad (27)$$

— ripples:

$$\frac{U}{U''_*} = A'_1 + B'_1 \log f''_t \quad (28)$$

$$A'_1 = -555 + 315 \log C \quad (29)$$

$$B'_1 = 25 \quad (30)$$

— anti-ripples:

$$\frac{U}{U''_*} = A''_1 + B''_1 \log f''_t \quad (31)$$

$$A''_1 = 100 + 40 \log C \quad (32)$$

$$B''_1 = -50 \quad (33)$$

The determination of A_1 , A'_1 , A''_1 is done by following a similar method used for the determination of α'_1 . Figure 16 indicates the rule of variation of coefficient A_1 . Representative points for sands and pumice have given accurate plottings. Only plottings corresponding to plastics presents a particularity due to the specific mass of the material. In fact, it was possible to show that the resistance of bed configurations decreases for increasing values of f''_t , when the bottom was covered by a light material. This means that, the law governing the resistance of bed configurations regenerated from materials such as plastics is somewhat different from natural sands. The influence of $\bar{\omega}$ on hydraulic characteristics of light material might be investigated carefully.

Determination of total bed resistance to flow

As a consequence of the above given study, the total bed resistance may be given as:

$$\frac{U}{U_*} = \frac{U}{U''_*} + \frac{U}{U''_*} \quad (34)$$

when f''_t is known, it becomes possible to evaluate U/U''_* , without ambiguity. But the determination



14/

of U/U''_* , presents some difficulty. In fact U/U''_* , differs according to the category of bed configuration. If the nature of the configuration can be predicted, U/U''_* , may be obtained directly from Figure 11.

Table 2 can be used for the predetermination of bed forms; but the limits given are not completely adequate. When $D \cong 0.55$ mm, it becomes difficult to predict the nature of the configurations. A method, given as follows, can be used in this case for the prediction of categories of bed configurations.

R''_t is taken as an independant variable.

Assume that R''_t , j , D , W , $\bar{\omega}$ are given and it is required to determine the category of bed configurations. When R''_t is known, f''_t can be computed as a function of the properties of bed materials. For $f''_t > f''_{t_0}$, dunes take place at the bottom surface (Fig. 17). But when $f''_t < f''_{t_0}$, two values of U/U''_* , are possible: one belonging to ripples the other to anti-ripples.

R''_t being known, U''_* , can be obtained immediately; in fact the slope "j" is a given data of the problem. Assuming that anti-ripples are formed on the bottom, a value of U/U''_* corresponds to a given value of f''_t . But U''_* , being known, U may be obtained from U/U''_* .

On the other hand, when U^3/gvj and U/\sqrt{gDj} are given, it becomes possible to compute U/U''_* , [8] or U'_t and R'_t as R'_t , f'_t and U/U'_t are known, the representative point of the flow in Figure 8 is already determined; if it falls over the representative straight line of the hydraulic system, anti-ripples are formed over the bed. If not, ripples might be considered.

In general, the geometry of the flow is known, so the depth "h" can also be measured. In that case, R can be computed. The values R''_t must be checked according to $R_t = R'_t + R''_t$. It is, in general, difficult to evaluate R''_t directly. When it is taken as an independant variable, as it was explained previously, the characteristics of the flow are completely determined. These might be reviewed following the above given expression, that is $R_t = R'_t + R''_t$. If the value of R_t so obtained is different from the measured value, R''_t might be changed and the computation repeated.

Conclusion

The mechanics of bed formations presents many properties which are explained in detail. It is believed that the difference in the velocities of sand particles and configurations cause the change in wave forms. The geometry of waves is summarized as follows:

- Downstream slope of waves: changes between 40° and 52° with the horizontal for ripples and is practically constant and equal to 33 ~ 35° for dunes (sand No. 2);
- Upstream slope of waves:
 - 20° for ripples,
 - 8° for dunes.

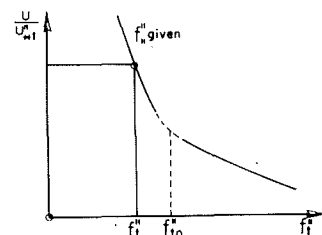
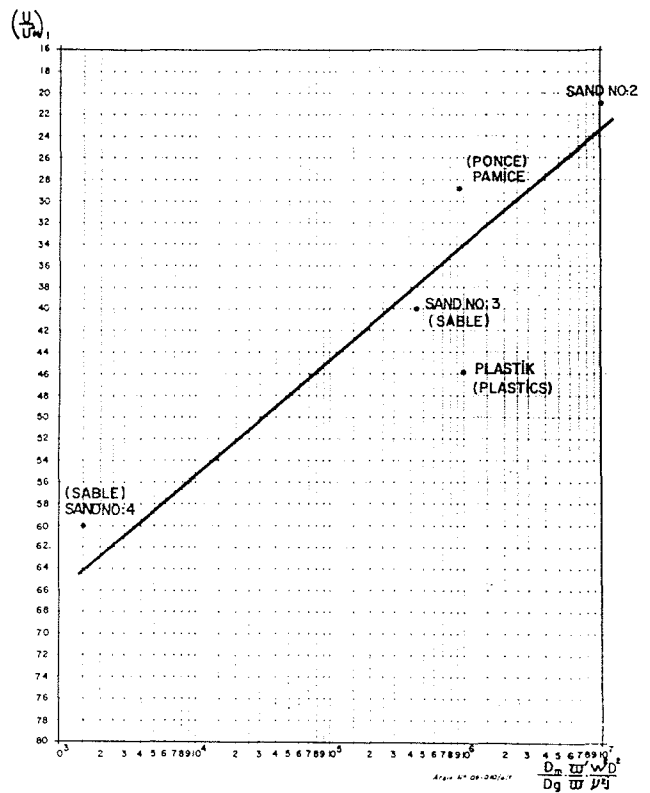
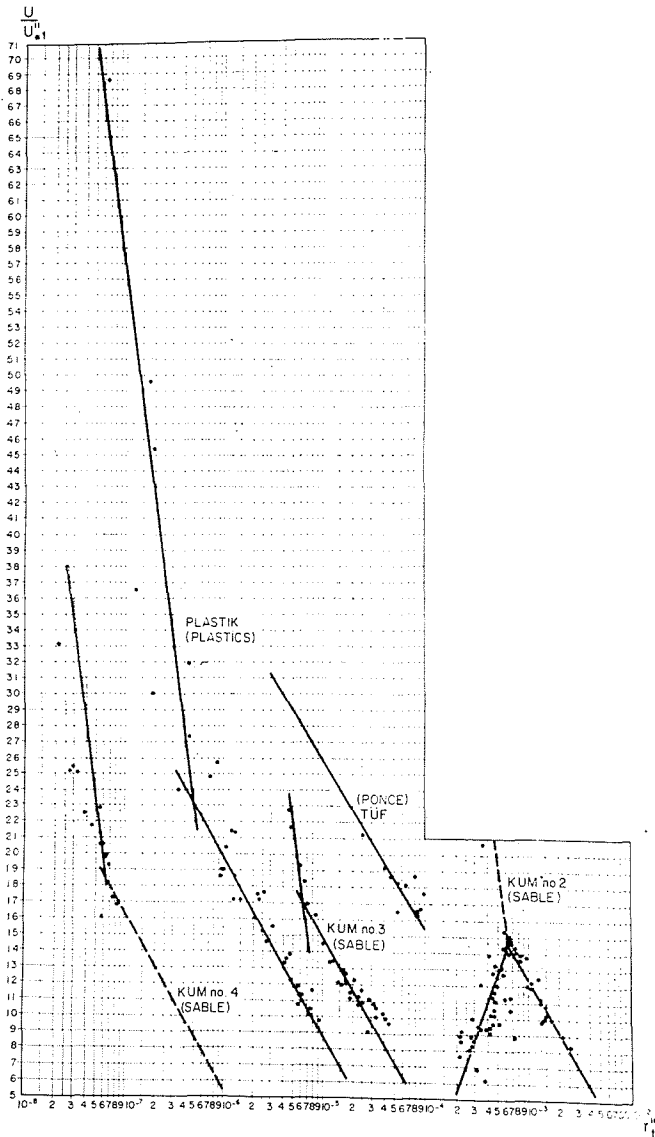
The velocity of waves changes with:

- The category of configurations;
- The depth of water;
- The friction velocity related to bed configurations.

It decreases gradually, becomes equal to zero and then takes negative values in case of anti-dunes. The bed resistance is a function of bed configurations and can be studied in four distinct groups:

- No. 1 : Plane bed, ripples, dunes;
- No. 2 : Plane bed, anti-ripples, dunes;
- No. 3 : Plane bed, dunes;
- No. 4 : Anti-dunes.

Each group presents a particular trend which governs the resistance.



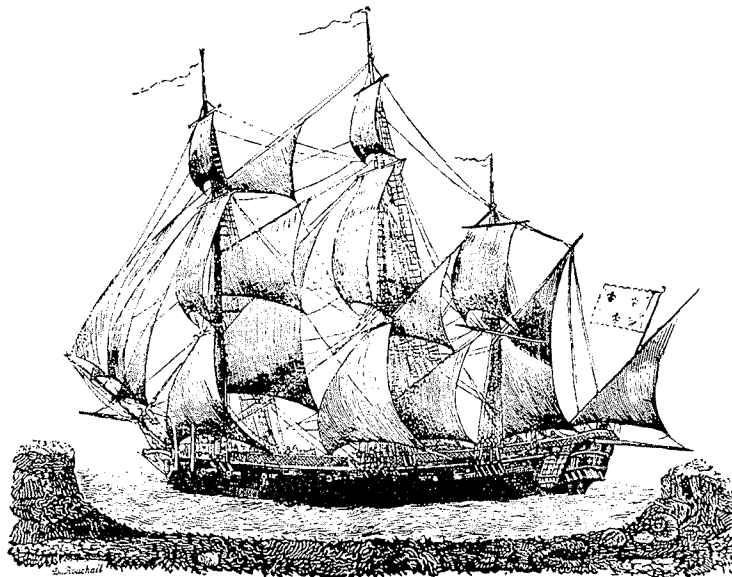
List of symbols

- D characteristic grain size;
 f friction parameter;
 f' friction parameter related to sand grains;
 f'' friction parameter related to bed configurations;
 f'_t friction parameter related to sand grains and measured at the bottom;
 f''_t friction parameter related to bed configurations and measured at the bottom;
 g gravitational acceleration;
 j hydraulic slope;
 R total hydraulic radius;
 R' hydraulic radius related to sand grains;
 R'' hydraulic radius related to bed configurations;
 R'_t hydraulic radius related to sand grains and measured at the bottom;
 R''_t hydraulic radius related to bed configurations and measured at the bottom;
 U mean velocity;
 U friction velocity;
 U' friction velocity related to sand grains;
 U'' friction velocity related to bed configurations;
 U''_* friction velocity related to sand grains and measured at the bottom;

- U''_* friction velocity related to bed configurations and measured at the bottom;
 W fall velocity of grains;
 \bar{w} submerged unit weight of grains;
 τ shearing stress at the bottom;
 ν kinematic viscosity of water.

References

[1] SENTÜRK (F.). — Tabii Akarsularda Taban Direncinin ve Taban Şekillerinin Hidrolik Karakteristikler Yönünden Tarifi ve İncelenmesi. *TBTAK. MAG*, 13, A (1967).
 [2] VANONI (V. A.) and NOMICOS (G. N.). — Resistance Properties of Sediment Laden Streams. *Proceedings ASCE* (May 1959).
 [3] LIU (H. K.). — Mécanisme de la formation des rides d'alluvion (French translation). *Proceedings ASCE* (Sept. 1957).
 [4] ANDAL (H. Einstein). — River Channel Roughness. *ASCE, Transactions*, vol. 117 (1952).
 [5] KEULOGAN (G. H.). — Laws of Turbulent Flow in Open Channels. Research paper, RP 1151, Bureau of Standards, vol. 21, p. 707-741.
 [6] SENTÜRK (F.). — Phénomène d'hystérésis dans les écoulements à fond mobile. Research paper, DSI.
 [7] SENTÜRK (F.). — La résistance de fond des écoulements étudiée en fonction d'un nouveau paramètre f appelé paramètre de friction. *C.R. Acad. Sci. Paris*, t. 260 (11 janvier 1965), p. 408-411.
 [8] SENTÜRK (F.). — Nehir Hidrologinde Benzemesim. *DSI* (1964).



Gravure du XIX^e siècle